

# Modeling of Deformable Thin Parts for Their Manipulation

Shinichi Hirai, Hidefumi Wakamatsu, and Kazuaki Iwata

Dept. of Mechanical Engineering for Computer-Controlled Machinery,  
Osaka University, Osaka 565, Japan

## Abstract

*A systematic approach to modeling of deformable soft parts for their manipulation is presented. Various deformable parts such as cords, leather products, and sheet metals are manipulated and are handled in a lot of manufacturing processes. Deformation of these parts is often utilized in order to manipulate them successfully while the manipulation sometimes fails because of unexpected deformation of the parts. Modeling of deformable objects is thus required so that the shape of the soft parts can be analyzed and can be evaluated on a computer.*

*In this paper, we will develop an analytical method to model the shape of a deformable object. Especially, we deal with deformation of a bendable thin object. Firstly, the process of manipulating a deformable object is analyzed with regard to how the object interacts with other objects around it. Secondly, model of a bendable thin object is formulated according to a principle that the potential energy of the object reaches to the minimum at its stable shape. Thirdly, algorithm to compute the deformed shape of the object is developed by applying a nonlinear programming technique. This algorithm is applied to some examples to show how it works. Finally, a simple experiment is done to demonstrate the validity of the modeling method proposed in this paper.*

## 1 Introduction

In the past decades, solid modeling techniques have been developed in design and manufacturing area. Solid modeling systems have a capability of handling the shape of rigid objects on a computer and many design and manufacturing processes have been automated by utilizing the modeling systems [1]. Most of manufacturing processes that deal with deformable soft objects such as rubber tubes, sheet metals, cords, leather products, and paper sheets are, however, still done by human workers. Automatic handling and manipulation of deformable objects are eagerly required. Manipulative operations of deformable objects are often performed by utilizing their deformation actively while the operations may result in failure because of unexpected deformation of the objects during the manipulation process. Modeling of deformable objects is thus necessary so that we can evaluate the shape deformation of soft parts on a computer and can derive task strategies that carry out manipulative operations successfully.

Automatic handling of deformable parts in shoe and garment manufacturing have been studied by many researchers [2]. These studies have been, however, done for individual processes independently and no systematic approaches have been developed yet. Some analytical approaches have been also studied toward a systematic approach. Zheng et al. have analytically developed a strategy that achieves the insertion of a soft peg into a hole [3]. Villarreal and Asada have proposed a concept of buffer zones that describe distributed compliance of the mated parts and have developed a method to derive task strategies using the buffer zones [4].

Solid modeling techniques have been applied to the studies on manipulation of rigid objects so that the model of the manipulated objects can be built. Thanks to the solid modeling techniques, a systematic approach to the manipulation of rigid objects has been developed recently. On the contrary, we have no systematic method of modeling deformable objects during their manipulative operations. Solid mechanics has been studied for a long time in order to analyze deformation of a solid body by investigating the relationship between stress and strain of the object [5]. It is not easy to analyze large deformation of a soft object such as paper and leather by solid mechanics approach, which basically deals with small deformation of a solid body. In computer graphics area, shape modeling of cloth objects has been proposed [6], and deformation of elastic objects has been studied [7]. These studies are not applicable to manipulative operations of deformable objects directly, since manipulation processes are not investigated in these studies.

In this paper, we will develop a systematic approach to the modeling of deformable objects for their manipulation. Especially, we will investigate the deformation of a bendable thin object such as paper and a sheet metal. Firstly, the process of manipulative operations is analyzed with regard to how a deformable object contacts with other objects around it. Secondly, the potential energy of the deformable object and the geometric constraints imposed on it are formulated in order to compute the deformed shape of the object by solving these equations. Thirdly, a numerical method to derive the deformed shape is developed by applying a nonlinear programming technique. Finally, an experimental result is shown in order to demonstrate the validity of the approach proposed in this paper.

## 2 Manipulation Process of Deformable Parts

Manipulative operations such as grasping and part-mating of deformable soft objects are often performed by utilizing deformation of the objects. For example, bending the object is one strategy to pick up a thin deformable object such as paper and a sheet metal on a flat horizontal table. Deformation of the object sometimes brings on the failure of manipulative operations. It is thus necessary to analyze the deformation of the object caused by the interaction with other objects during the manipulation process so that we can evaluate if the deformation is appropriate to achieving the manipulative operation.

Manipulation process of rigid objects can be modeled as a series of transitions among contact states between the objects to be mated [8]. At individual contact states, the geometric constraints imposed on the manipulated object differ significantly one another and the control strategy of object motion is thus different. Manipulation process of a deformable soft object can be regarded as a series of state transitions as well. For example, an operation to pick up a thin object on a flat horizontal table consists of a series of transitions among four states, as shown in Figure 1. At individual states, the geometric constraints imposed on the object differ significantly one another, that is, boundary conditions are different from one another. Thus, individual states are corresponding to different fundamental operations, which cause deformation and motion of the object. State (b) shown in the figure is, for example, corresponding to the operation of bending the object by applying forces to it while state (d) describes the operation of lifting the object by moving fingertips upward. Transitions from one state to another state are corresponding to fundamental operations that change the geometric constraints imposed on the object. Transition from state (a) to state (b) is, for example, corresponding to the operation of contacting fingertips to the object while transition from state (c) to state (d) expresses the operation of releasing the fingertips from the object. Manipulation process of deformable objects can be, therefore, modeled as a series of fundamental operations.

## 3 Modeling Bend Deformation of Thin Objects

### 3.1 Basic Principle

As mentioned in the previous section, manipulation process of a soft object can be regarded as a series of fundamental operations that cause deformation and motion of the object. Especially, deformation operations are key to successful manipulation of the deformable object. Deformed shape of a soft object strongly depends upon the direction and the magnitude of forces applied to it, the geometric constraints imposed on it by other objects, material properties of the object under a variety of environments around it, and so on. That is, deformed shape of the object is intensively related to physical properties of the object and the environment. It is thus necessary to derive

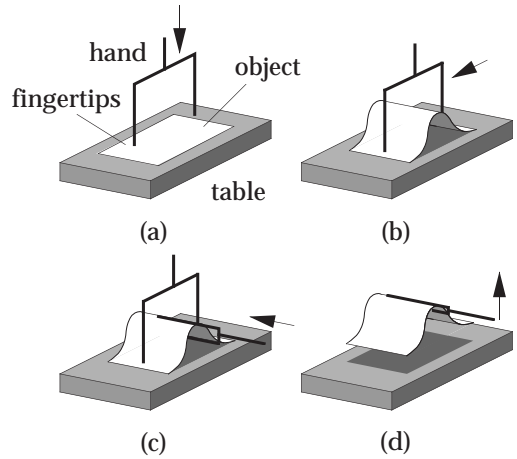


Figure 1: Process of pickup operation

deformed shape of the object based on physical models of the object, the environment, and the interaction between them.

In this paper, we will adopt a basic principle that the potential energy of a deformable object reaches to the minimum under the geometric and physical constraints imposed on it at its stable deformed shape. We will ignore dynamical effects during a bending operation. In the following sections, we will investigate the uniform bend deformation of a thin object such as paper and a sheet metal.

### 3.2 Formulation of Potential Energy and Geometric Constraints

In this section, we will formulate the potential energy of a bendable thin object and the geometric constraints imposed on it. We assume that a thin object on a horizontal table is deformed uniformly, as shown in Figure 2. Let  $L$  be the length of the object,  $s$  be the distance from one end point of the object along it, and  $\theta(s)$  be the angle from the horizon at coordinate  $s$ . As shown in the figure, take the  $x$ - and  $z$ - axes in the horizontal direction and in the vertical direction, respectively. Coordinates  $x$  and  $z$  corresponding to distance  $s$  is then describe as follows, respectively:

$$x(s) = \int_0^s \cos \theta ds + x_0, \quad (1)$$

$$z(s) = \int_0^s \sin \theta ds + z_0 \quad (2)$$

where  $x_0$  and  $z_0$  denote  $x$ - and  $z$ - coordinates at the left end point of the object, respectively. We assume that potential energy of the object  $U$  is given by the sum of elastic energy  $U_{bend}$  and gravitational energy  $U_{grav}$ . Namely,

$$U = U_{bend} + U_{grav}. \quad (3)$$

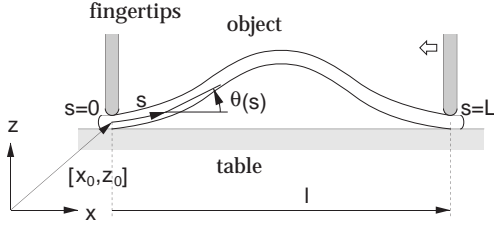


Figure 2: Bend deformation of thin object

Assuming that bend moment at an arbitrary point of the object is proportional to the curvature at that point, elastic energy  $U_{bend}$  is given by

$$U_{bend} = \int_0^L \frac{1}{2} D \dot{\theta}^2 ds \quad (4)$$

where  $\dot{\theta}$  is the derivative of function  $\theta$  with respect to coordinate  $s$  and  $D$  denotes the bend rigidity of the object, which is assumed to be constant. Gravitational energy is describe by

$$U_{grav} = \int_0^L Agz ds \quad (5)$$

where  $A$  denotes mass per unit length of the object and  $g$  represents the acceleration of gravity.

Due to the interaction between a thin object and other objects such as fingertips and a table, some geometric constraints are imposed on the object. Let us derive the geometric constraints imposed on the object. Contact between the object and the fingertips yields some geometric constraints. Let  $\theta_0$  and  $\theta_L$  be the angles from the horizon at both end points, respectively. Then, we have

$$\theta(0) = \theta_0, \quad \theta(L) = \theta_L. \quad (6)$$

Let  $l$  be the distance between the end points of the deformed object. Since the distances between the end points along  $x$ - and  $z$ - axes are given by  $l$  and  $0$ , respectively, we have the following equations:

$$x(L) = x_0 + l, \quad z(L) = z_0 \quad (7)$$

Contact between the object and the table yields other geometric constraints. Note that any points on the object must be located over the horizontal table or on it. This condition is described as follows:

$$z(s) \geq z_0 \quad \forall s \in [0, L] \quad (8)$$

Computing function  $\theta(s)$  that minimizes potential energy  $U$  described as eq.(3) under geometric conditions given by eqs.(6), (7), and (8), we can derive the

deformed shape of a bendable thin object. Namely, computation of the deformed shape results in a variational problem. Note that the geometric constraints imposed on an object consist of not only equational conditions such as eqs.(6) and (7) but also inequality conditions, for example, eq.(8). Condition that an object is not interfered with other objects is described by a set of inequalities, since mechanical contacts between the objects constraints the object motion unidirectionally.

## 4 Computation of Deformed Shape

### 4.1 Computation Algorithm

Computation of the object shape results in a variational problem as mentioned in the previous section. One method to solve a variational problem is Euler's approach, which is based on the stationary condition in function space. In Euler's approach, equational conditions are embedded into the objective function using Lagrange's undetermined coefficients, and the object shape can be obtained by solving Euler's differential equations. This approach has, however, the following drawbacks:

- Inequality conditions cannot be taken into account.
- Differential equations are often difficult to solve them.

Conditions that individual objects are not interfered with one another are mathematically described by inequalities such as eq.(8), that is, the geometric constraints resulting from mechanical contacts are unidirectional. Note that these constraints are nonholonomic [9]. The shape of an object that minimizes potential energy thus does not necessarily satisfy the stationary condition. This implies that Euler's approach, which is based on the stationary condition, is not applicable.

In this paper, we will develop a direct method based on Ritz's method [10] and a nonlinear programming technique. Let us express function  $\theta(s)$  by a linear combination of basic functions  $\varphi_1(s)$  through  $\varphi_n(s)$ :

$$\theta(s) = \sum_{i=1}^n a_i \varphi_i(s) \triangleq \mathbf{a}^T \boldsymbol{\varphi} \quad (9)$$

where  $\mathbf{a} = (a_1, a_2, \dots, a_n)$  is a vector consisting of coefficients and  $\boldsymbol{\varphi} = (\varphi_1, \varphi_2, \dots, \varphi_n)$  is a series of basic functions. Substituting eq.(9) into eq.(3), potential energy  $U$  is described by a function of coefficient vector  $\mathbf{a}$  as follows:

$$U(\mathbf{a}) = \int_0^L \frac{1}{2} D (\mathbf{a}^T \dot{\boldsymbol{\varphi}})^2 ds + \int_0^L Ag \left\{ \int_0^s \sin(\mathbf{a}^T \boldsymbol{\varphi}) ds \right\} ds. \quad (10)$$

The geometric constraints given by eqs.(6), (7), and (8) are also described by conditions concerning coefficient vector  $\mathbf{a}$ . In addition, discretizing eq.(8) by

dividing interval  $[0, L]$  into  $N$  small intervals yields a finite number of conditions. As a result, a set of the geometric constraints is expressed as follows:

$$\mathbf{a}^T \boldsymbol{\varphi}(0) = \theta_0, \quad \mathbf{a}^T \boldsymbol{\varphi}(L) = \theta_L \quad (11)$$

$$\int_0^L \cos(\mathbf{a}^T \boldsymbol{\varphi}) ds = x_0 + l, \quad (12)$$

$$\int_0^L \sin(\mathbf{a}^T \boldsymbol{\varphi}) ds = z_0 \quad (12)$$

$$\int_0^{\frac{kL}{N}} \sin(\mathbf{a}^T \boldsymbol{\varphi}) ds \geq z_0 \quad (13)$$

$$\forall k = 0, 1, \dots, N$$

We can determine the deformed shape of an object by computing coefficient vector  $\mathbf{a}$  that minimizes the potential energy  $U$  expressed by eq.(10) under the geometric constraints given by eqs.(11), (12), and (13). This minimization problem under equality and inequality conditions can be solved by use of a nonlinear programming technique such as multiplier method [11]. The deformed shape of the object corresponding to coefficient vector  $\mathbf{a}$  can be computed by use of eqs.(1) and (2).

## 4.2 Numerical Examples

In this section, some numerical examples are shown in order to demonstrate how the proposed method computes the deformed shape of a bendable thin object. The first example demonstrates that the shape of the object with large deformation can be computed simply by use of the proposed method. The second example shows how gravity has an effect on the deformed shape. The third example shows the deformed shape of the object surrounded by some obstacles. The following set of basic functions are used in the computation of these examples:

$$\boldsymbol{\varphi} = (\varphi_1, \varphi_2, \varphi_3, \varphi_4, \varphi_5)$$

$$= \left(1, \sin \frac{2\pi s}{L}, \cos \frac{2\pi s}{L}, \sin \frac{4\pi s}{L}, \cos \frac{4\pi s}{L}\right). \quad (14)$$

Assume that the length of the object  $L$  is equal to 100 in the following examples.

The first example shows the object shapes computed for some values of  $l$ , which denotes the distance between the end points of the deformed object. Table 1 describes the computational result of coefficients  $a_1$  through  $a_5$  and potential energy  $U$  with respect to some values of distance  $l$ ; 90, 70, 50, 30. In this example, potential energy of the object is assumed to be equal to its bend energy, that is, gravitational energy of the object is neglected. Both angles from the horizon at the end points of the object  $\theta_0$  and  $\theta_L$  are assumed to be 0(rad). As shown in the table, coefficients except  $a_2$  are equal to zero. Namely, the deformed shape in this example can be characterized coefficient  $a_2$ , which is corresponding to base function  $\varphi_2$ . Figure 3 illustrates the deformed shapes computed from coefficients listed in the table. The proposed method

Table 1: Example of computed coefficient vector and potential energy

$l$	$a_1$	$a_2$	$a_3$	$a_4$	$a_5$	$U$
90	0.000	0.641	0.000	0.000	0.000	0.041
70	0.000	1.141	0.000	0.000	0.000	0.129
50	0.000	1.521	0.000	0.000	0.000	0.228
30	0.000	1.869	0.000	0.000	0.000	0.345

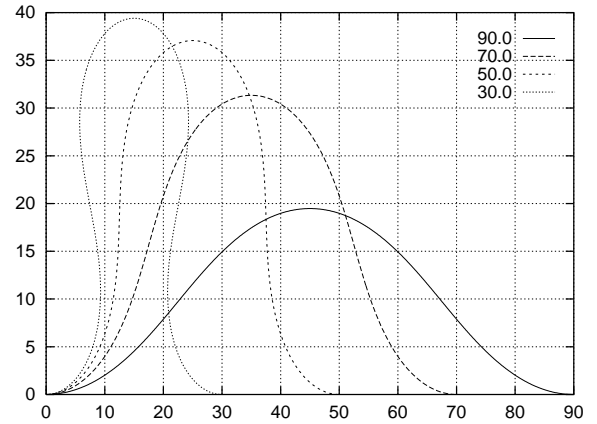


Figure 3: Example of computed object shape

has a capability of computing the shape for a thin object with large deformation, as shown in the figure. We find that the deformed shape is symmetry with respect to an axis along the  $z$ -axis. Note that coefficients  $a_1$ ,  $a_3$ , and  $a_5$ , which are corresponding to even functions  $\varphi_1$ ,  $\varphi_3$ , and  $\varphi_5$ , respectively, are equal to zero. This implies that the deformed shapes are axial symmetry.

The second example demonstrates the computation of the object shape considering the gravitational energy. Normalizing the potential energy and the geometric constraints by means of dividing variable  $s$  by length  $L$ , we find that the shape of the object is determined by the following dimensionless quantity:

$$\rho = \frac{Ag}{D} L^3 \quad (15)$$

Quantity  $\rho$  represents the contribution of the gravitational force to the shape of an object. Especially, the gravitational force is neglected at  $\rho = 0.0$ . Table 2 describes the computational result of the coefficients and the potential energy with respect to various values of  $\rho$ ; 0.0, 1.0, 2.0, 3.0, 5.0 ( $\times 10^3$ ). The distance between the end points  $l$  is fixed to 70 and both angles from the horizon at these points  $\theta_0$  and  $\theta_L$  are equal to 0(rad). As shown in the table, coefficients  $a_3$  and  $a_5$ , which corresponding to even functions  $\varphi_3$  and  $\varphi_5$ , respectively, are nonzero when quantity  $\rho$  exceeds  $2.0 \times 10^3$ . This implies that the deformed shape of the object is not axial symmetric.

Table 2: Example of computed coefficient vector and potential energy considering gravity

$10^{-3}\rho$	$a_1$	$a_2$	$a_3$	$a_4$	$a_5$	$U$
0.0	0.000	1.141	0.000	0.000	0.000	0.129
1.0	0.000	1.135	0.000	-0.130	0.000	0.281
2.0	0.000	1.074	-0.004	-0.420	0.005	0.417
3.0	0.000	0.900	0.462	-0.332	-0.462	0.518
5.0	0.000	0.672	0.673	0.000	-0.673	0.702

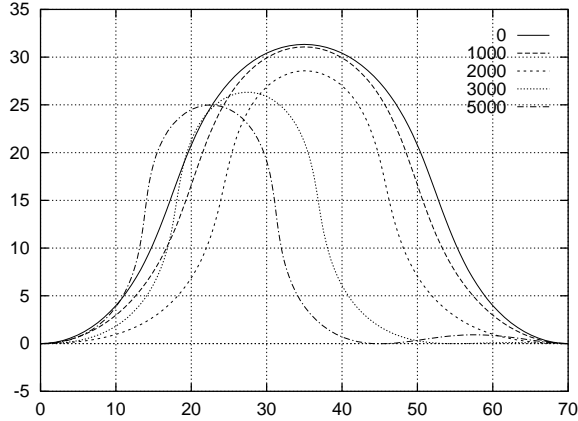


Figure 4: Example of computed object shape considering gravity

The deformed shapes of the object corresponding to coefficients listed in the table are shown in Figure 4. As shown in the figure, the height of the object decreases with increasing quantity  $\rho$ . In addition, the deformed shape is not symmetric any more when  $\rho$  exceeds  $2.0 \times 10^3$ . Note that we have two shapes symmetric each other with respect to the central vertical line in these cases. One shape of the two is illustrated in the figure. In order to verify that the unsymmetric shape minimizes the potential energy, let us compute the coefficient vector and the potential energy of the object assuming that the object shape is symmetric. Potential energy  $U$  is, for example, equal to 0.746 at  $\rho = 3.0 \times 10^3$  assuming that the deformed shape is symmetric, while the minimum value of potential energy is equal to 0.518 as shown in the table. Namely, the symmetric shape does not satisfy the condition that the potential energy reaches its minimum at a stable deformed shape. This implies that deformed shapes are unsymmetric when dimensionless quantity  $\rho$  exceeds a certain value.

The third example shows the computed shape of a deformable object surrounded by obstacles. Note that the condition that objects are not interfered with one another can be described by a set of inequalities such as eq.(8), since kinematic constraints imposed on an object by mechanical contact with the other objects are unidirectional. The deformed shape of an object

Table 3: Example of coefficients describing shape of object surrounded by obstacles

$a_1$	$a_2$	$a_3$	$a_4$	$a_5$	$U$
-0.046	0.419	-0.483	0.817	0.529	0.415

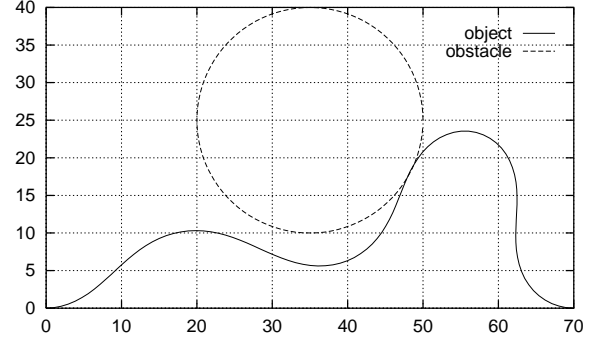


Figure 5: Example of object shape among obstacles

surrounded by obstacles can be derived by use of the proposed method due to its capability of taking inequality conditions into account. Table 3 provides the coefficients and the potential energy describing the deformed shape of a thin object surrounded by a circular obstacle with its center at coordinates (35.0, 25.0) and with radius 15. The shape of the object is shown in Figure 5. As shown in the figure, the object is deformed with contacting to the obstacle and the deformed shape is unsymmetric.

## 5 Experimental Result

In this section, we will show an experimental result of the shape measurement in order to demonstrate the validity of the proposed method. Let us measure the deformation of a sheet of copy paper 200(mm) long, 30(mm) wide, and 92( $\mu$ m) thick. The bend rigidity  $D$  and the weight  $Ag$  per unit length of the paper are  $10^4(gw \cdot mm^2)$  and  $2 \times 10^{-3}(gw/mm)$ , respectively. The paper is deformed so that the distance  $l$  be 180, 140, and 70(mm). Measurement values of the deformed paper and the computational values by the proposed method are plotted in Figure 6. The solid and the dotted lines represent the computational result and the measured values, respectively. In the computation, we assume that angles  $\theta_0$  and  $\theta_L$  are equal to zero. Quantity  $\rho$  turns out to be equal to 1.60. This implies that the gravitational energy is neglectable in the computation. The difference between the computed values and experimental values along  $z$ -axis is 11(mm) at most. The ratio of the difference to the length of the paper is approximately 6%.

The difference between the computed shapes and the measurement values results from the discrepancy between the given values and the actual values of angles  $\theta_0$  and  $\theta_L$ . From the measurement values, we estimate that angles  $\theta_0$  and  $\theta_L$  are actually equal to

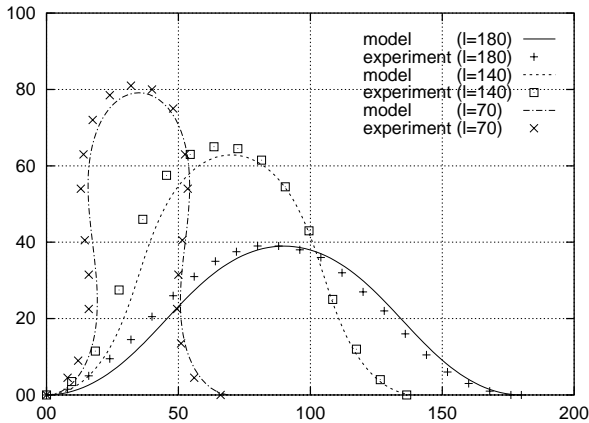


Figure 6: Comparison between computed values and measured values

$10^\circ$  and  $0^\circ$ , respectively. The computed values using the estimated angles are illustrated in Figure 7. The difference between the computed values and experimental values along  $z$ -axis is 2(mm) at most. Namely, the ratio of the difference to the paper length is reduced to 1%. As a result, we conclude that the proposed method is appropriate to the deformed shape modeling of a copy paper.

## 6 Concluding Remarks

An analytical approach to the modeling of deformable objects for their manipulation has been developed based on the physical properties of the objects. Firstly, process of manipulating a deformable object was modeled as a series of fundamental operations. We found that some fundamental operations cause deformation and motion of the object whereas the other operations change the geometric constraints imposed on the object. Secondly, the potential energy of an object and the geometric constraints imposed on it were formulated. We found that the geometric constraints consisted of inequality conditions as well as equational conditions. The deformed shape of the object can be derived by minimizing the potential energy under the geometric constraints. Thirdly, an algorithm that derives the object shape was developed by applying a nonlinear programming technique. We have demonstrated that the shape of the object with large deformation surrounded other objects can be computed using the proposed algorithm. Finally, a simple experiment was done in order to demonstrate the validity of the proposed approach. We have shown that deformed shape of a copy paper can be modeled appropriately by use of the proposed method.

Using the modeling technique proposed in this paper, we can analyze and can evaluate the deformed shape of a uniform thin object under various environments on a computer. This enables us to plan manipulative operations such as handling and part-mating that deal with these deformable parts.

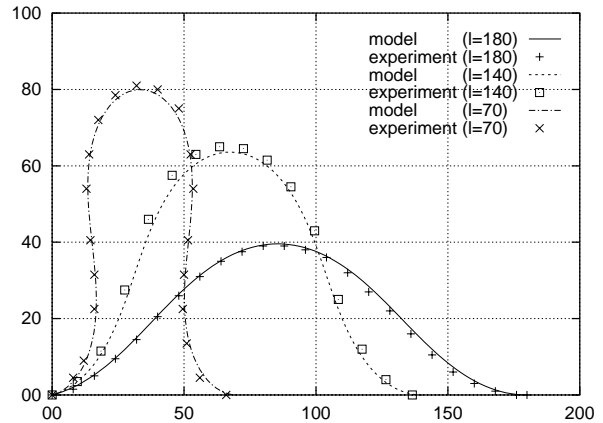


Figure 7: Computational values using estimation of actual angles from horizon at end points

## References

- [1] Mäntylä, M., *An Introduction to Solid Modeling*, Computer Science Press, 1988
- [2] Taylor, P. M. et al., *Sensory Robotics for the Handling of Limp Materials*, Springer-Verlag, 1990
- [3] Zheng, Y. F., Pei, R., and Chen, C., *Strategies for Automatic Assembly of Deformable Objects*, Proc. IEEE Int. Conf. Robotics and Automation, pp.2598–2603, 1991
- [4] Villarreal, A. and Asada, H., *A Geometric Representation of Distributed Compliance for the Assembly of Flexible Parts*, Proc. IEEE Int. Conf. Robotics and Automation, pp.2708–2715, 1991
- [5] Fung, Y. C., *Foundations of Solid Mechanics*, Prentice-Hall, 1965
- [6] Weil, J., *The Synthesis of Cloth Objects*, Computer Graphics, Vol 20, No.4, pp.49-54, 1986
- [7] Terzopoulos, D. et al., *Elastically Deformable Models*, Computer Graphics, Vol 21, No.4, pp.205-214, 1987
- [8] Desai, R. S. and Volz, R. A., *Identification and Verification of Termination Conditions in Fine Motion in Presence of Sensor Errors and Geometric Uncertainties*, IEEE Int. Conf. Robotics and Automation, pp.800–807, 1989
- [9] Goldstein, H., *Classical Mechanics*, Addison-Wesley, 1980
- [10] Elsgolc, L. E., *Calculus of Variations*, Pergamon Press, 1961
- [11] Avriel, M., *Nonlinear Programming: Analysis and Methods*, Prentice-Hall, 1976